Fishing Ban

Haishan Yuan*

University of Queensland

October 11, 2023

Abstract

China has implemented the world's first large-scale seasonal fishing bans for sustainable fishery, but their effectiveness is unclear given the challenges of patrolling a vast ocean. Using a novel dataset of marine vessels recorded at night and a regression discontinuity in time design, we find that the bans reduce boat detections in China's Exclusive Economic Zone (EEZ) by about 72%, and the subsequent lifting of the fishing ban increased the number of boat detections by about 78%. However, there is no spatial discontinuity around the EEZ border, and more boats are detected inside the Chinese EEZ near its border with the Vietnamese EEZ when the Chinese fishing bans are effective. Since the Vietnamese EEZ was more intensively fished than the nearby Chinese EEZ, this spatial pattern near the EEZ border suggests that Vietnamese fishermen fished in the Chinese EEZ during the ban periods.

Keywords: Tragedy of the Commons; Regression Discontinuity in Time or Space; Fishing Ban; Fishery; Exclusive Economic Zone (EEZ); EEZ Incursion.

JEL Classification Numbers: Q22, Q56, Q58, K42, O13

*Address: Level 6, Colin Clark Building (39), University of Queensland, St Lucia, QLD 4072, Australia; Email: h.yuan@uq.edu.au; I thank Hee-Seung Yang, Youjin Hahn, and the participants at the KDI-3ie Conference on Impact Evaluation in Development Research, Monash Environmental Economics Workshop, and Australasian Development Economics Workshop for their helpful comments. All errors are mine. Disclosure: I do not have significant competing financial, professional, or personal interests that might have influenced the work described in this manuscript.

1 Introduction

Fisheries and aquaculture provide livelihoods to 10% to 12% of the world's population (U.N. Food and Agriculture Organization, 2014). In 2014, 38 million people were directly employed in fisheries. 80% of motorized fishing vessels were in Asia (U.N. Food and Agriculture Organization, 2016). Being the country with the most fishermen and the largest fishing fleet, China alone had over 5.75 million fishery workers in 2015, including 3 million traditional fishermen[1] (China Fishery Statistical Year Book, 2016). However, the Food and Agriculture Organization (FAO) of the United Nations estimates that about one third (31.4%) of world fish stocks in 2013 were fished at a biologically unsustainable level, with another 58.1% of stocks were fully fished, leaving only 10.5% of stock underexploited (U.N. Food and Agriculture Organization, 2016).

Overfishing is a classical example of the Tragedy of the Commons, where Coasian solutions are not feasible, and government regulations are needed. To reduced overfishing, China has implemented the world's first large-scale seasonal fishing bans. For two to four months each year in the summer, commercial fishing is prohibited in the Chinese Exclusive Economic Zone (EEZ). Given the difficulties in patrolling a vast ocean, it is unclear whether such fishing bans are effective. Moreover, given the usual difficulties in measuring illicit activities, direct evidence on the effectiveness of fishing regulation is very limited. In this paper, I answer this question using a novel dataset on boats detected offshore at nights. The dataset is derived from remote sensing imagery from the new-generation weather satellite program.

Using a regression discontinuity in time design (RD in time), I find that the start of fishing bans reduced the number of boat detections by about 72% and the subsequent lifting of fishing ban increased the detected boats by 78%. I found no spatial discontinuity around the EEZ border. Moreover, around the China-Vietnam EEZ border in the Gulf of Tonkin (a.k.a. Beibu Bay), where the Vietnamese side of the gulf is more intensively fished than the Chinese side, the density of boat detections at nights are higher on the Chinese side when the Chinese fishing bans were effective than when the bans

[1] In 2015, 20% Chinese fishery workers are women. In this paper, fishermen refer to both men and women in the fishery.

were not in effect. The opposite is true for the outer Chinese EEZ border outside of the Gulf of Tonkin, where is further offshore and the inside of Chinese EEZ is more intensively fished than the outside. The lack of spatial discontinuity at the border, along with the spatial patterns of detected boat density around the EEZ border during and outside of the fishing ban periods, suggests that the exclusivity of fishing activities to the nationals of the EEZs are not strictly enforced at the EEZ border. EEZ incursions take places close to the border of Chinese EEZ, both by Chinese and non-Chinese fishing vessels.

This paper contributes to a large literature on the policies for the conservation of the environment and natural resources (see Cropper and Oates, 1992 and Brown, 2000 for a review). To the best of my knowledge, this paper is the first to empirically investigate the effectiveness of the Chinese summer fishing ban, which is the first large-scale regulatory policy for a sustainable fishery in a developing country or in the form of seasonal complete ban on commercial fishing.

The literature on environmental conservation policies has found that subnational inter-jurisdictional spillovers are important in considering a national policy on environmental conservation (see, e.g., Burgess et al., 2012; Lipscomb and Mobarak, 2016). The literature also documents important spillovers of environmental regulation (and enforcement thereof) across firms (Chan and Zhou, 2021), and the relocation of economic activities due to environmental regulation (Walker, 2011; Carruthers and Lamoreaux, 2016).

My findings suggest that, in the context of the sustainable marine fishery, international spillover in regulatory policy also affects the effectiveness of environmental regulation. My findings echos with what Sigman (2002) called international free-riding in regulating pollution of transnational river systems.

This paper also contributes to the growing literature that uses remote sensing data to measure and study environmental conditions and economic activities (see, e.g., Henderson et al., 2012; Michalopoulos and Papaioannou, 2013; Hodler and Raschky, 2014; Lipscomb and Mobarak, 2016; Chan and Zhou, 2023, and Donaldson and Storeygard, 2016 for a review). In particular, Assunção et al. (2023) studied the use of a re-

mote sensing system to monitor and enforce conservation efforts in the Brazilian Amazon, where illegal logging was widespread due to weak institutional protection for the environment. They found that the remote sensing system in Brazil greatly facilitated effective environmental monitoring and regulation enforcement against deforestation. Given that the implementation and enforcement of environmental regulations critically depend on monitoring and measurements (Lipscomb and Mobarak, 2016; He et al., 2020), the findings in this paper highlight the promising potential of using remote sensing data for enforcing environmental regulations.

Flückiger and Ludwig (2015) and Axbard (2016) found that negative income shocks from fishery increase piracy, which induced violence and substantial welfare losses, including by interrupting shipping routes (Besley et al., 2015). In light of these studies, our findings suggest that fishing bans may have both short-run and long-run effects on piracy across regions.

The rest of the paper is organized as follows. In the next section, I discuss the background of seasonal fishing ban policy and then present our main findings on the effectiveness of the Chinese fishing bans in Section 4. Evidence of EEZ incursions are presented in Section 5. Section 6 concludes.

2 Background

2.1 Fishing Ban: Why?

Since the Economic Reform in the late 1970s, fishery in China has grown rapidly. Now, China has the world's largest fishery workforce and fishing fleet. According to the China Fishery Statistical Year Book (2016), 20 million Chinese rely on fishery for their livelihood, and 14 million workers are employed directly or indirectly in fisheries. There were just above one million fishing vessels in 2016, among which two-thirds were motorized fishing vessels. 272 thousand motorized fishing vessels operate in the sea, 69% of which are small vessels less than 12 meters long (see Table 1 for the number and share of Chinese seafaring fishing vessels by size).

Table 1: Number of Seafaring Fishing Vessels by Size

	Number		Tonnage	
Less than 12 meter	186,781	68.6%	882,361	10.0%
12 meter to 24 meter	49,697	18.2%	1,919,347	21.8%
24 meter or longer	35,844	13.2%	5,989,801	68.1%
Total	272,322	100%	13.838,949	100%

Notes: Data as of the end of 2015 from the China Fishery Statistical Year Book (2016).

While total marine catches increases by many folds since the Economic Reform, many fish stocks declined quickly. In the 1980s and early 1990s, China implemented a number fishery management policy, including a fishing vessel registration and licensing system and resource fee collection scheme. However, these measures did not seem adequate. Starting from the mid-1990s, China has imposed a seasonal fishing ban, along with other policies aiming at reducing the capacity of fishing fleets.[2]

2.2 Fishing Ban: When?

China first officially introduced a seasonal fishing ban in the Yellow Sea and the East China Sea in 1995. In 1999, the summer fishing ban was extended to the South China Sea, covering most of China's marginal seas in the Pacific. In 2009, the Chinese Ministry of Agriculture further extended the duration of summer fishing ban. The duration of the annual fishing ban varies for different marine areas. But most recently in 2017, the Ministry of Agriculture synchronize the starting date of the annual fishing ban to an early date of May 1st, while leaving the ban period to end at different dates for different marine zones.

As detailed in the following section, we focus on the sample period from 2012 to 2017 due to data availability. Table 2 displays the effective dates of annual fishing bans from 2009 to 2017 for various Chinese marine zones. Prior to 2017, the duration of fish-

[2]It should be noted that many have argued that official statistics of marine catches have been misreported. In particular, marine catches had been over-reported since the mid-1990s (Watson and Pauly, 2001), which suggested that the over-fishing and collapsing speed of fishery stock in Chinese EEZ may be underestimated based on reported marine catches. Indeed, FAO has treated the Chinese fishery statistics with caution and separated them from those from the rest of world (FAO, 2002).

ing bans ranged from 2.5 to 3.5 months. Since 2017, the fishing bans in each zone have been expanded, now ranging from 3.5 to 4.5 months during the summers, representing the most extensive bans since their introduction in 1995.

Table 2: Effective Dates of Fishing Bans

Zone Number	Zone Description	Years 2009 – 2016		Year 2017 onward	
		Start Date	End Date	Start Date	End Date
1	Northern Yellow Sea (North of N 35°)	June 1st	September 1st	May 1st	September 1st
2	Southern Yellow Sea and Northern East China Sea (between N 35° and N 26°30′)	June 1st	September 16th	May 1st	September 16th
3	Southern East China Sea (between N 26°30′ and Min-Yue marine boundary)	May 16th	August 1st	May 1st	August 16th
4	Taiwan Strait and South China Sea (between Min-Yue maritime boundary and N 12°)	May 16th	August 1st	May 1st	August 16th

Notes: This table lists the start and end dates of fishing bans in each zone for different years. In descending order from the north, Zone 1 is the northernmost, and Zone 4 is the southernmost. The text in each zone corresponds to the same color coding as shown on the map in Figure 1, which illustrates the geographic extents of these zones in our analysis. There were minor exceptions in Zones 2 and 3 regarding certain fishing methods.

2.3 Fishing Ban: Where?

According to the United Nations Convention on the Law of the Sea, China has sovereign rights to the marine resources below the surface of the sea within its Exclusive Economic Zones (EEZs). An EEZ covers the sea zone from the coastal baseline to 200 nautical miles outward (approximately 370.4 kilometers or 230 miles) unless it overlaps with a 200-nautical mile zone of another nation. In such cases, conventionally, the midpoints of the maritime areas between two nations' coastal baselines determine the outward boundary of an EEZ. China's fishing bans, therefore, apply to its EEZs.

In Figure 1, I plot the EEZs for each marine zone with fishing bans as listed in Table 2. The Paracel Islands in the South China Sea are controlled and claimed by China, but their sovereignty is disputed by the governments of Vietnam and Taiwan. The Spratly Islands are claimed by China, Indonesia, Malaysia, the Philippines, Taiwan, and Vietnam. All of these governments, except Indonesia, also control parts of the Spratly Islands. China's maritime claims in the South China Sea further conflict with those of Brunei. Additionally, China, Taiwan, and Japan claim uninhabited islands respectively named Diaoyudao Islands, Diaoyutai Islands, and Senkaku Islands. These disputed islands are located to the northeast of Taiwan and to the west of Okinawa Island.

Figure 1: Zones of Fishing Ban

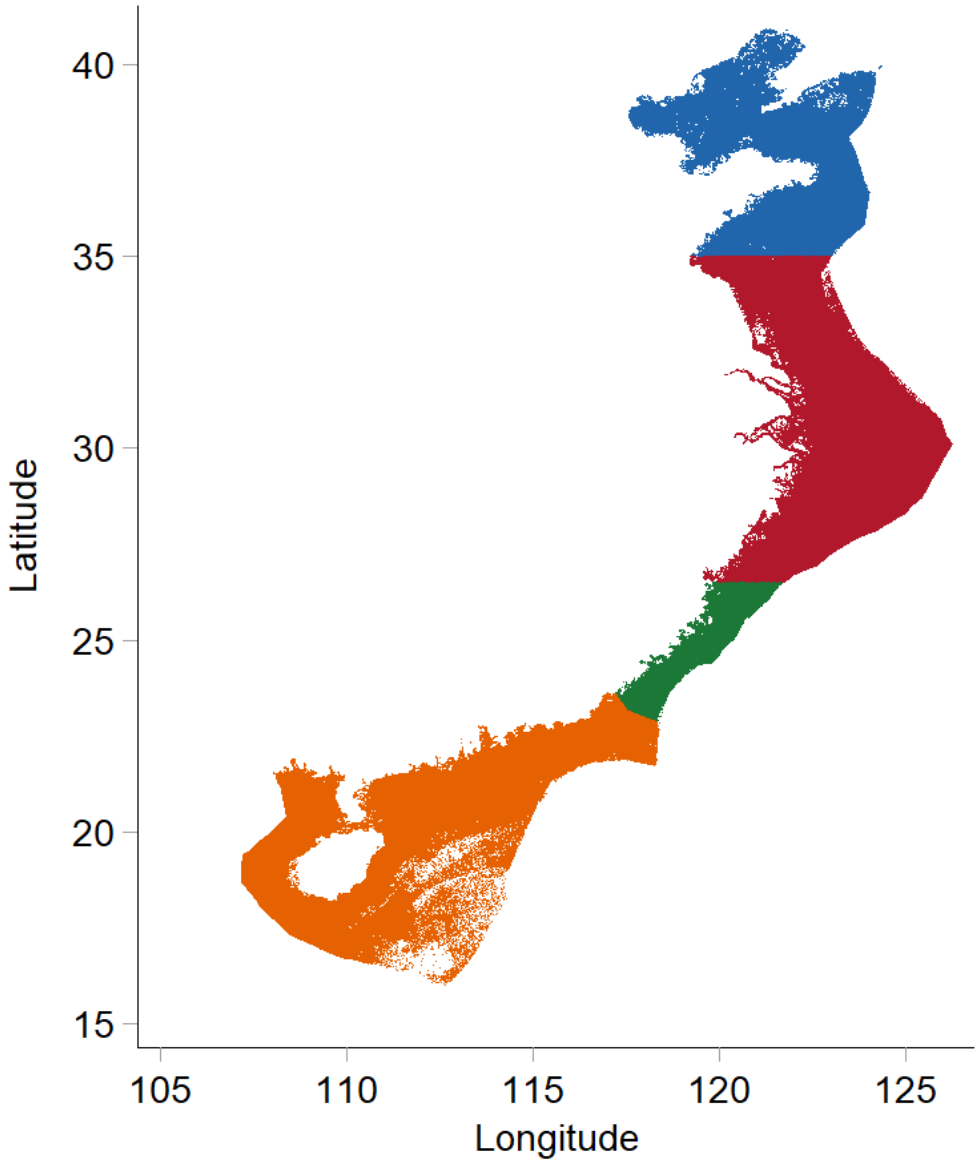

Notes: This figure plots the Exclusive Economic Zones (EEZs) for each marine zone with fishing bans listed in Table 2. From top (north) to bottom (south), the four zones are Zones 1 to 4 and share the same color coding as indicated in Table 2.

Due to the complications arising from these sovereignty disputes, I have excluded the EEZs claimed by China that are derived from the sovereignty of these disputed islands in my analysis in this paper. Moreover, I have also excluded the EEZs claimed by China that are derived from islands controlled by the Taiwan authorities. Throughout this paper, I refer to Taiwan as a geographic area or its government without implying any particular legal status. Similarly, I refer to China as the authority of the People's Republic of China (P.R.C.) or as a geographic area where the P.R.C. maintains effective and undisputed control.

Figure 2 plots the undisputed and disputed EEZs of China and its neighbors in the Northwest Pacific Ocean. I obtain Geographic Information Systems (GIS) data from the organization Marine Regions and use the Version 8 World EEZ Boundaries data published in 2014.

2.4 Fishing Ban: How?

The vast ocean makes it challenging to patrol and enforce fishing bans. During fishing ban periods, the China Coast Guard, in collaboration with provincial ministries of fisheries, conducts patrols and inspections of fishing vessels. Violations of the fishing ban may result in prosecutions. For instance, in 2017, Chinese agencies conducted patrols covering over 800,000 nautical miles, inspected 76,000 fishing vessels, issued fines for 2,764 fishing ban violations (including more than 100 criminal prosecutions), and confiscated 800 tons of fish and 89,000 meters of fishing nets (Ministry of Agriculture, 2017).

China adopted a zero-growth policy to control fishing capacity in 1999 and has implemented a strict licensing policy for fishing vessels. During fishing ban periods, fishery authorities inspect fishing ports for unregistered vessels and violations of the fishing ban by both registered and unregistered vessels. In some regions, fishermen are also required to surrender their fishing tools during the fishing ban. In recent years, the Chinese government has provided modest subsidies to fishermen during the fishing ban period for income maintenance.

Figure 2: Exclusive Economic Zones in the Northwest Pacific

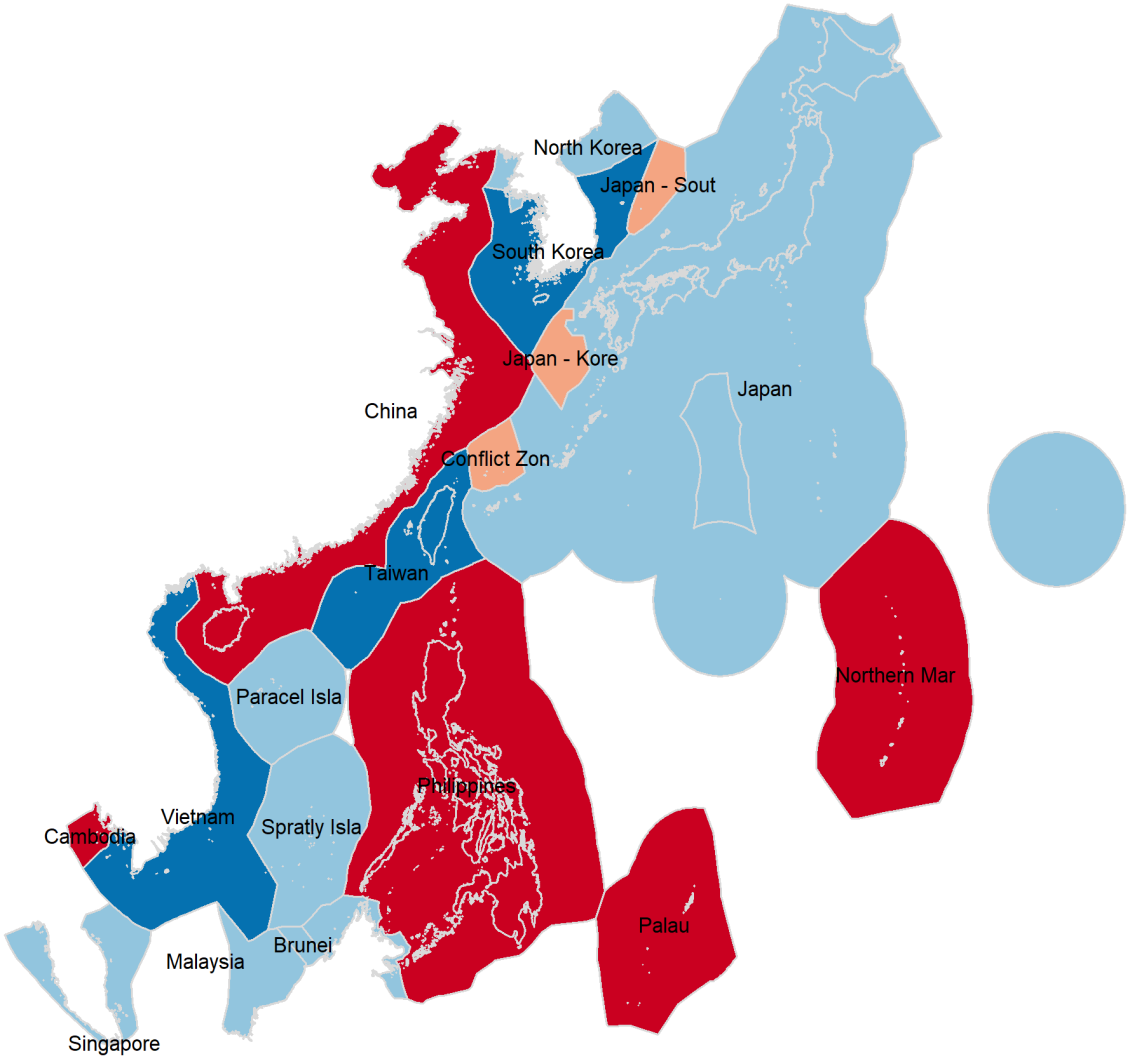

Notes: This figure plots the undisputed and disputed EEZs of China and its neighbors in the Northwest Pacific Ocean using the Version 8 World EEZ Boundaries data from the organization Marine Regions.

3 Data Description

3.1 VIIRS Boat Detection Data

The primary data in this paper is the VIIRS Boat Detection (VBD) data from the National Oceanic and Atmospheric Administration (NOAA). The VIIRS Boat Detection (VBD) project is jointly sponsored by the U.S. Agency for International Development and NOAA, using remote sensing images from the Suomi National Polar-orbiting Partnership satellite.

A collaborative program between NOAA and the Atmospheric Administration (NOAA), the Joint Polar Satellite System (JPSS) is the new generation polar-orbiting operational environmental satellite system in the U.S. Established in 2011, the JPSS will replace the U.S. Air Force's Defense Meteorological Satellite Program (DMSP), and Suomi NPP is the first satellite launched under the JPSS. The second one, JPSS-1, was launched in November 2017.

Most existing economic studies using remote sensing data have relied on data derived from satellite images from the DMSP-OLS program.[3]

The VIIRS Boat detection data are derived from the images captured by the Visible Infrared Imaging Radiometer Suite (VIIRS), which is the primary imager on Suomi NPP. Compared to the imaging sensors suite in DMSP Operational Linescan System (DMSP-OLS), VIIRS provides high-quality remote sensing imagery in terms of spatial resolution and the ability to detect weak light sources. For comparison, Nighttime DMSP-OLS pixels have a 5 km × 5 km footprint, while the VIIRS Day/Night Band sensor unit has a 742 m × 742 m footprint. The low-light imaging detection limit is about 5×10^{-10} Watts/cm^2/sr for DMSP-OLS and 2×10^{-11} Watts/cm^2/sr for VIIRS. In short, VIIRS Day/Night Band offers about 45 times finer spatial resolution and is 25 times more sensitive in low-light imaging detection than DMSP-OLS (Elvidge et al., 2013).

Moreover, as suggested by its name, VIIRS is capable of collecting imagery and radiometric measurements of the Earth's surface and atmosphere in the visible and

[3]See Donaldson and Storeygard (2016) for a review of this literature.

infrared bands of the electromagnetic spectrum. This capability enables the distinction of light emitted from human activities, such as fishing boats and LED lights, from sources like gas flares in oil mines and explosions in war zones (Elvidge et al., 2015b).

Since 2000, fishery agencies in Japan, Korea, Thailand, and Peru have been granted permission to use DMSP-OLS data for fishery management with at least a 3-hour delay. However, the limited ability of DMSP-OLS to detect low light at fine spatial resolutions and the absence of automatic algorithms for boat detection have constrained the utility of satellite images for fishery management. The VIIRS Boat Detection project has significantly advanced the use of satellite imagery for fishery management by developing an automatic boat identification system using images from the VIIRS Day/Night Band (DNB), which consists of sensors adapted to a wide wavelength spectrum.

In a nutshell, the VBD algorithm detects spikes in illumination from offshore areas in the DNB images while controlling background noise radiance caused by moonlight. It also filters out recurring light sources (such as features on land) and energetic particles in the upper atmosphere (ionosphere) that can affect electromagnetic sensors. The algorithm further classifies boat detections as either strong or weak by comparing the spikes to neighboring pixels. Additionally, it uses the spectral characteristics of a spike to identify and label gas flares, such as those from offshore drilling stations. For more in-depth information about the algorithms, please refer to Elvidge et al. (2015a), which also includes a validation study demonstrating that the algorithm correctly identified 99.3% of the reference pixels. These reference pixels were chosen from a set of 594 boats visually identified by an analyst and an additional 245 pixels that were not initially identified by the analyst.

Given that the boat detection is a product of remote sensing imagery, the ability to detect boats is considerably affected by the prevailing weather in a location. Although the algorithm adopted a sharpness index to rate the sharpness of features and identify detection that is affected by clouds, dense clouds, rains, and storms limit the ability for the remote sensing to capture night light and hence detect light emitted by boats. Moreover, the sensors and algorithm are most capable of detecting offshore boats at night with new moon, where the oceans are less lit by moonlight. In full moon nights,

the algorithm could have false identifications of boats due to the brightness variations in clouds.

However, despite its limitations, the VBD data offers a unique dataset of offshore boats at a high frequency across an extensive spatial scale. The VBD data is available for most Exclusive Economic Zones (EEZs) in Asia, Oceania, North America, and select European countries. Notably, the VBD data covers all of China and its neighboring countries' EEZs. Since the Suomi NPP scans the same location twice, once around noon and again around 1:30 AM local time, the VBD data provides daily (nightly) boat identifications at a fine spatial resolution across a vast geographic area.

3.2 Boats at Night

The VBD data analyzed in this paper spans from February 2nd, 2012, to December 31, 2017. I have retained both strong and weak boat detections and excluded blurry detections, gas flares, glows, recurring lights, and offshore platforms. Aggregating all the boat detections over my sample period, I plotted the spatial density of boat detections in a heatmap in Figure 3. The heatmap covers China's Exclusive Economic Zone (EEZ) and neighboring seas at a spatial resolution of 1 degree of latitude and longitude, which correspond to approximately 110 km (68 miles) vertically and 100 km (62 miles) horizontally.[4]

As seen in Figure 3, the marine areas near the shore are generally brighter than international waters or EEZs farther away from the shore. The brightest spots, representing areas with the densest detected boats, are near the shores close to Beijing, Tianjin, Shanghai, Hong Kong, and Guangzhou, which are the largest cities in China. Each bin or cell in the heatmap is a hexagon, with an area of approximately 7100 km^2. The areas with the densest boat detections have as many as 200,000 detections per cell, or close to 28 detections per square kilometer over 4.75 years.

Figure 4 contains a similar heatmap but with a much smaller spatial resolution. Now, each hexagon spans 0.1 degrees of latitude and longitude, covering an area of

[4] 1 km is approximately equal to 0.627 mile, and 1 mile is approximately equal to 1.609 km; 1 nautical mile is equal to 1.852 km.

approximately 71 square kilometers. The areas with the densest boat detections have as many as 10,000 detections per cell, or close to 140 detections per square kilometer over 4.75 years. Additionally, there are several bright spots near the Shandong Peninsula, which is surrounded by the Yellow Sea in eastern China around N 37°, and near the Liaodong Peninsula, which is also surrounded by the Yellow Sea in northern China around N 40°.

Outside of China's EEZ, we can observe that the nearshore areas are quite bright around the southern Korean Peninsula. In particular, there is a well-defined bright area surrounding Jeju Island, which is the largest island in South Korea and the Korean Peninsula. The marine area off the Vietnam coast also exhibits a swath of boat detection, consistent with the fact that this area is among the world's most over-fished regions (U.N. Food and Agriculture Organization, 2014). Figure 4 suggests significant spatial variation in fishing intensities, with some areas clearly serving as fishing grounds.

Figure 3: Boats at Night

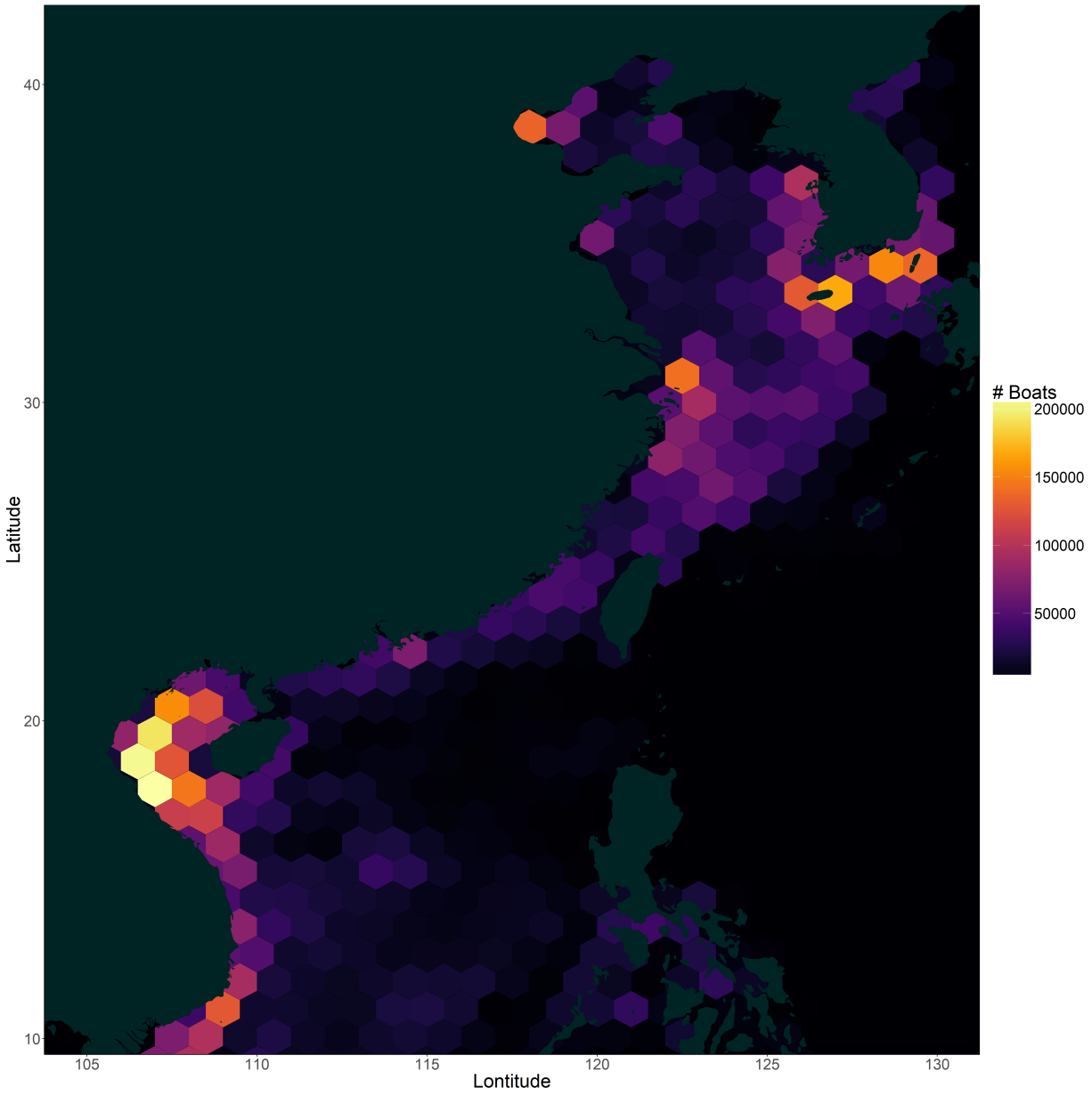

Notes: Each hexagonal area in the heat map above is color-coded to represent the total number of boat detections from April 2nd, 2012 to December 31, 2017. The geographic extent is given by the horizontal axis for longitude (E) and the vertical axis for latitude (N). The horizontal and vertical span of a hexagon are both 1 degree or approximately 100 km.

Figure 4: Boats at Night

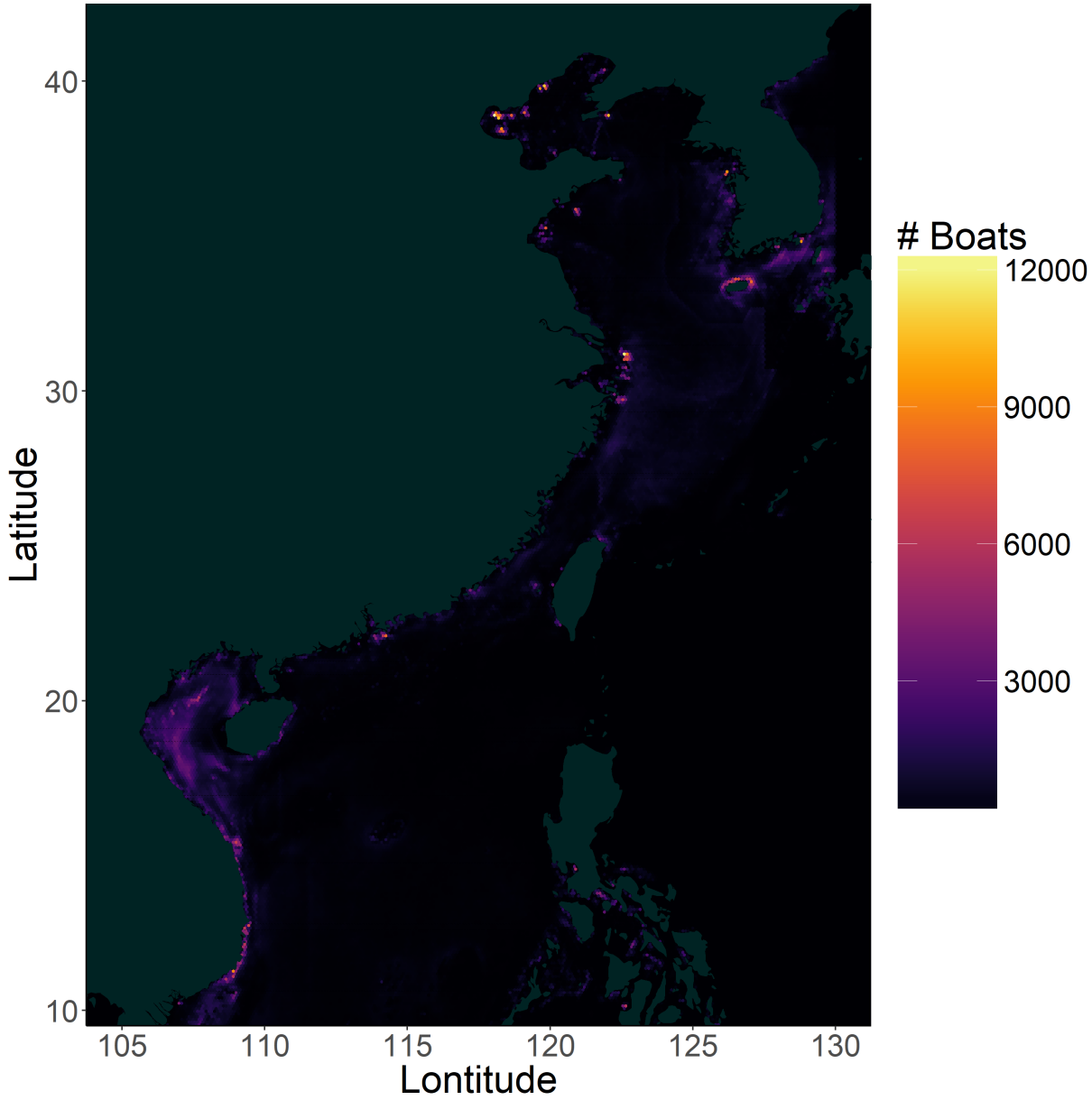

Notes: Each hexagonal area in the heat map above is color-coded to represent the total number of boat detections from April 2nd, 2012 to December 31, 2017. The geographic extent is given by the horizontal axis for longitude (E) and the vertical axis for latitude (N). The horizontal and vertical span of a hexagon are both 0.1 degree or approximately 10 km.

4 The Effectiveness of Fishing Bans

In this section, we propose two empirical approaches to study whether China's summer fishing bans reduce the number of boat detections in the Chinese Exclusive Economic Zones (EEZs). In the first approach, we parametrically control for seasonal variations in the number of boats and estimate the effects of fishing bans using an indicator variable that signifies whether the fishing ban is effective on date t. Our second approach employs a nonparametric regression discontinuity in time (RD in Time) design.

For both empirical approaches, we exploit the time series variation in the fishing ban policy across different regulatory zones. First, I aggregate all boat detections in each regulatory zone, as shown in Figure 1 and described in Tables 2, into nightly aggregates. For each zone z, I estimate the following specifications:

$$Y_{zt} = \gamma_z B_{zt} + f_z(t) + \delta_z' X_t + \epsilon_{zt} \tag{1}$$

where Y_{zt} is the total number of boat detections on night z in natural logarithm; B_{zt} is an indicator variable equal to one if a fishing ban is effective for zone z on night t; $f_z(t)$ is a polynomial of day of the year, ranging from 1 to 366; X_t is a set of control variables to be explained below; ϵ_{zt} is an error term; and γ_z and δ_z are zone-specific coefficients.

Table 3 presents estimates of γ_z for each zone, starting from Zone 1 to Zone 4, as shown from top to bottom. In Column (1), the polynomial $f_z(t)$, which accounts for seasonal variations in boat detections, is quadratic; in Column (2), the polynomial $f_z(t)$ is cubic. Columns (3) and (4) also provide specifications with quadratic and cubic polynomials, respectively, while including fixed effects for both the day of the week and the day of the lunar month.

The inclusion of lunar month fixed effects accommodates variations in moonlight, which can affect the technical capability of satellite imagery to detect boats. Day of the week fixed effects are included to account for any potential impacts on fishermen's work schedules due to weekends and weekdays. However, it is worth noting that statistically significant day-of-the-week effects appear to be rare.

Heteroskedasticity-and-autocorrelation robust standard errors, following Newey and West (1986), are reported in parentheses, with a maximum lag of serial correlation set at 35 nights.

As indicated in Table 3, the summer fishing bans had substantial and consistently negative impacts on boat detections in Zone 1 and Zone 4. In Zone 1, the fishing ban reduced boat detections by 64.7 to 70.4 logarithmic points, essentially halving the number of detections, depending on the specification used. In Zone 4, located in the South China Sea, the fishing ban similarly resulted in a reduction of boat detections by 70.2 to 70.4 logarithmic points, again amounting to a halving of detections. These estimates, derived from the eight specifications, all exhibit statistical significance at the 1% level.

In the case of Zone 2, the coefficient estimates are consistently negative in all four specifications. However, statistical significance is observed only at the 5% level in Column (2) and at the 10% level in Column (4). In these specific specifications, the fishing ban leads to a reduction in Zone 2's boat detections by approximately 28% to 35%.

As for Zone 3, the coefficients are relatively small and exhibit negativity in two of the specifications. None of the coefficients are precisely estimated or reach statistical significance at the conventional levels.

One advantage of our first approach is that, if the parametric specification is correct, the estimates should be efficient and provide the average treatment effects of fishing bans on boat detections. However, if the parametric assumptions are not approximately correct, perhaps due to misspecified polynomials or omitted variables, the estimates may be biased. To address these concerns, I will employ a nonparametric RD in Time design, also known as the interrupted time series method (see Davis, 2008; Chen and Whalley, 2012; Anderson, 2014; Auffhammer and Kellogg, 2011 for examples, or Hausman and Rapson, 2018 for a review of this method). The identification assumption for nonparametric identification with RD in time is that the time trend would move smoothly in the absence of treatments, such as fishing bans in this context.

To implement the RD in time design, I separately examine two phases: when the fishing bans become effective and when they are lifted. Fishing bans during our sample period began at noon. For each regulatory zone and year from 2012 to 2017, I normalize

Table 3: Fishing Ban and the Number of Boats Detected: by Zone

	(1)	(2)	(3)	(4)
	Zone 1			
Fishing Ban Effective	-0.647***	-0.704***	-0.661***	-0.692***
	(0.132)	(0.136)	(0.118)	(0.118)
Obs.	2035	2035	2035	2035
	Zone 2			
Fishing Ban Effective	-0.181	-0.438**	-0.148	-0.325*
	(0.225)	(0.210)	(0.209)	(0.188)
Obs.	2008	2008	2008	2008
	Zone 3			
Fishing Ban Effective	-0.141	0.079	-0.099	0.216
	(0.248)	(0.203)	(0.251)	(0.206)
Obs.	1660	1660	1660	1660
	Zone 4			
Fishing Ban Effective	-0.740***	-0.742***	-0.702***	-0.718***
	(0.133)	(0.134)	(0.116)	(0.119)
Obs.	2031	2031	2031	2031
Day of the Year	Quadratic	Cubic	Quadratic	Cubic
Day of the Week	-	-	Indicators	Indicators
Day of the Lunar Month	-	-	Indicators	Indicators

Notes: This table reports the parametric estimates of fish ban on the log number of boat detections. Panels 1 to 4 from the top represent estimates for Zones 1 to 4 respectively. The specifications in Columns (1) and (3) include a quadratic term of the day of the year to control for seasonal effects. The specifications in Columns (2) and (4) include a cubic term of the day of the year to control for seasonal effects. The specifications in Columns (3) and (4) additionally include day of the week indicators and day of the lunar month indicators. Newey and West (1986) heteroskedasticity-and-autocorrelation robust standard errors are reported in the parentheses, where the maximum lag of serial correlation is 35 nights.

* $p < 0.10$; ** $p < 0.05$; *** $p < 0.01$.

the first night after the ban takes effect to be zero. The running variable is defined in non-negative terms as the number of nights since the fishing ban took effect and in negative terms as the number of nights before the fishing ban became effective.

I then aggregate the total number of boat detections by zone, year, and the running variable in nights. These aggregated data are subsequently pooled across zones and averaged by year. I focus on a window where the running variable, denoted as τ, falls within the range [-50, 50]. Consequently, the outcome variable Y_τ measures the total number of boat detections in China's EEZ τ nights after the fishing bans became effective (or $|\tau|$ nights before the bans took effect if $\tau < 0$).

Likewise, when analyzing the lifting of the fishing ban, I designate the first night after the ban is lifted as night zero and define the running variable accordingly.

To visually assess how the activation of fishing bans affects the number of boat detections, I have plotted the boat detections against the running variable in Figure 5. In this figure, each green circle represents the number of boat detections in China's EEZ τ nights after the fishing bans become effective, and the purple dashed lines represent local linear fits.

The average number of boat detections in China's EEZ gradually increases over the 50 days leading up to the commencement of the fishing bans, peaking at around 11,000 detections just a few days before the bans take effect. However, once the fishing bans become active, the number of boat detections experiences a sharp drop to approximately 4,000 per night.

Furthermore, we do not observe substantial increases shortly before the fishing bans become effective, which might be expected if fishermen were intensifying their fishing efforts in anticipation of the bans. The absence of clustering of activity just before the ban effective dates suggests that fishing in the month preceding the bans was likely already at or near full capacity or profit-maximizing intensity. Any further increases in fishing efforts may have been either unfeasible or unprofitable.

We also notice a drop in boat detections one night before the fishing bans. This drop is approximately half the size of the drop observed from two nights before the fishing ban to the first night of the ban. The decrease in boat detections before the ban

Figure 5: Fishing Ban On

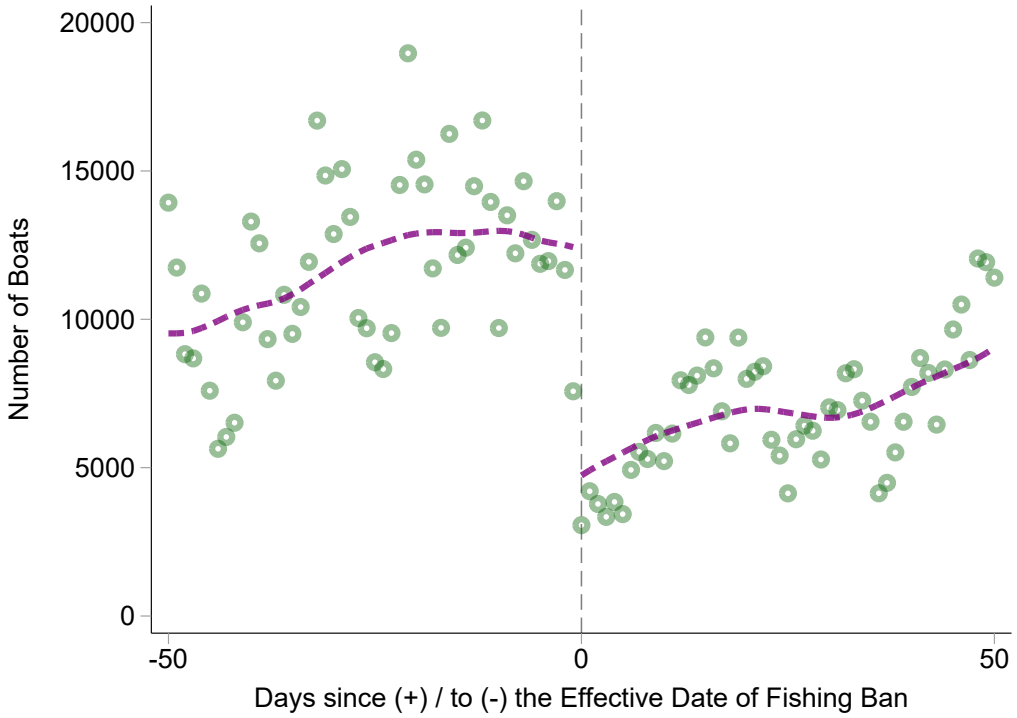

Notes: Each green circle represents the average number of boat detections across all China's EEZ τ nights since the fishing bans became effective for $\tau \geq 0$; or $|\tau|$ nights before the fishing bans became effective for $\tau < 0$. The purple dashed lines are local linear fits. Night 0 is the first night after the fishing bans became effective and the horizontal axis represents τ. The vertical axis represents the total number of boat detections.

suggests that fishing boats had already started returning to their harbors two nights before the fishing bans took effect.

It's important to note that the last observations before the fishing bans were recorded approximately 10.5 hours before the bans became effective, at a time when fishing vessels were required to have returned and docked in the harbors. Considering that a typical fishing cruise covers little more than 10 km per hour and the outer boundary of an EEZ can be up to 370 km offshore, with considerable uncertainties in estimated arrival time due to changing winds and currents, it's not surprising that cautious fishermen would return to the harbor before 1:30 AM on the same day the fishing ban started.

After the initial sharp decline following the implementation of fishing bans, boat detections gradually increase. There are a couple of potential explanations for this trend.

One possibility is that the weather during the ban months becomes progressively clearer, with fewer clouds and less rain, making it easier for satellite imagery and detection algorithms to identify boats at night.

Alternatively, the effectiveness of the fishing bans may erode over time, due to factors on both the demand and supply sides. On the demand side, as the ban period continues, the accumulation of unsatisfied seafood demand may grow, particularly for fresh seafood, as the bans can significantly reduce the seafood supply. Traditional holidays such as the Dragon Boat Festival, Chinese Valentine's Day, and the summer school holiday also fall within the ban period, likely increasing seafood demands.

On the supply side, the potentially higher prices of seafood during the fishing bans could incentivize more fishermen to engage in illegal fishing, especially those facing liquidity constraints and lacking alternative income sources during the bans. Additionally, as fish stocks recover from intensive fishing, the fishing yield for a fixed fishing effort may also increase.

If the fishing bans unraveled completely before their scheduled end date, we wouldn't observe a sharp increase in boat detections when the bans were officially lifted. On the other hand, if the bans remained effective, the incentive to evade the bans and engage in illegal fishing would be highest in the days leading up to their expiration. After a prolonged ban period, fish stocks would be at their peak, and there would be strong demand for seafood. Attempting to fish immediately after the bans were lifted could yield substantial profits (if not detected).

To further investigate this, I've created an RD graph akin to Figure 5, but this time, the focus is on the lifting of the fishing bans.

In Figure 6, I plot the number of boat detections per night in Chinese EEZs against the number of nights since or before the fishing bans were lifted. As the bans were lifted, there was a significant surge in boat detections. The number of detections increased from approximately 12,000 on the eve of the ban lifts to around 25,000 detec-

tions two nights after the bans were lifted. Interestingly, the increase on the first night after the ban lift was also roughly half of the drop from the eve of the ban lift to two nights later.

Figure 6: Fishing Ban Off

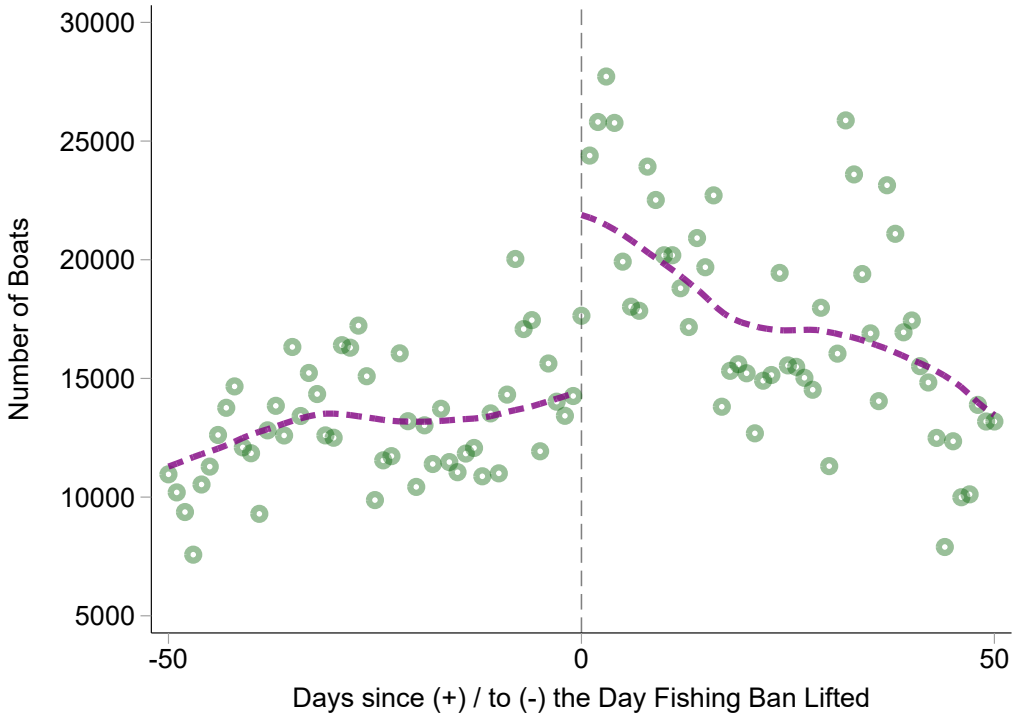

Notes: Each green circle represents the average number of boat detections across all China's EEZx τ nights since the fishing bans were lifted for $\tau \geq 0$; or $|\tau|$ nights before the fishing bans were lifted for $\tau < 0$. The purple dashed lines are local linear fits. Night 0 is the first night after the fishing bans were lifted and the horizontal axis represents τ. The vertical axis represents the total number of boat detections.

There were no clear upward trends in the nights leading up to the ban lifts, suggesting that illegal fishing might not have been widespread. Furthermore, following the ban lifts, the number of boat detections gradually declined. One possible reason for this decline is that increased fishing activity depleted fish stocks over time, reducing the profitability of fishing and leading to fewer operating fishing boats.

A visual examination of Figure 5 and Figure 6 suggests that fishing bans indeed had a substantial negative impact on boat detections in the Chinese EEZs. Table 4 presents

the nonparametric RD estimates using the bias-corrected local linear estimators introduced by Calonico et al. (2014).

Table 4: Nonparamatric RD Estimates of Fish Ban on the Number of Boats Detected

	Fishing Ban On		Fishing Ban Off	
	# Boats	log(# Boats)	# Boats	log(# Boats)
RD Estimate	-8228.098***	-1.290***	10014.657***	0.576***
	(1055.609)	(0.135)	(2462.001)	(0.146)
# Observations	151	151	151	151

Notes: This table reports the nonparametric RD estimates of fish ban on the number of detected boats. * $p < 0.10$; ** $p < 0.05$; *** $p < 0.01$.

The first two columns provide estimates of the local average treatment effects (LATEs) of imposing the fishing bans, with the outcome variable as either the number of boat detections or the logarithmic value of boat detections. The last two columns present similar estimates, but this time for the LATEs of lifting the fishing bans.

The RD estimate in the first column suggests that imposing the fishing ban lowered the number of boat detections by 8,228 per night in the Chinese EEZs. The log specification in the second column suggests that this corresponds to a reduction of 129 log points, or 72%, which is a substantial impact.

When the fishing bans were lifted, boat detections increased by 10,015 or 57.6 log points, representing a 78% increase. It's worth noting that the LATE estimates for the ban lifting are slightly less precise compared to those for imposition, which is not surprising. As observed in the RD graphs, there is somewhat more noise around the ban lifting compared to ban imposition.

However, all four LATE estimates are highly statistically significant, with each one reaching the 0.001% level of statistical significance.

While fishing bans had an impact on the number of boat detections across the Chinese EEZs, their effectiveness may vary in individual regulatory zones due to differences in local enforcement capabilities or measures. To examine how the fishing bans influenced each regulatory zone, I have presented RD graphs, similar to Figure 5 and Figure 6, separately for each zone in Figure 7.

Figure 7: RD in Time: Number of Boats per Night by Zone

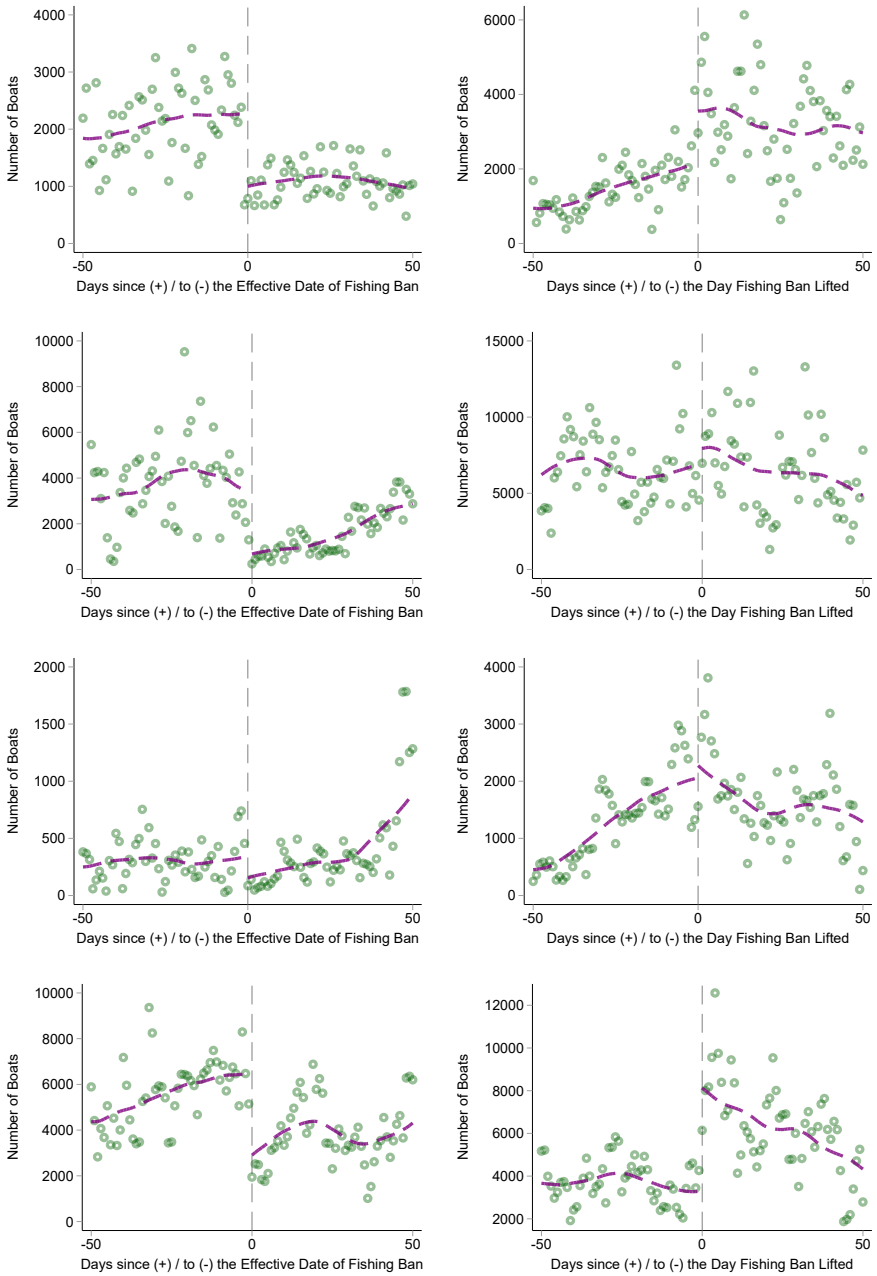

Notes: The RD graphs above are similar to Figure 5 and Figure 6 but separately for each zone. The subplots on the left hand size concern the starting of fishing bans; the subplots on the right hand size concern the lifting of fishing bans. Rows 1 to 4 represents Zones 1 to 4 respectively. Each green circle represents the average number of boat detections across all China's EEZx τ nights since (+) or before (-) the fishing bans became effective (left subplots) or were lifted (right subplots). Night 0 is the first night after the fishing bans were lifted and the horizontal axis represents τ. The vertical axis represents the total number of boat detections.

The subplots on the left-hand side of Figure 7 resemble Figure 5 and pertain to the initiation of fishing bans, while the subplots on the right-hand side resemble Figure 6 and concern the lifting of fishing bans. Rows 1 to 4 represent Zones 1 to 4, respectively.

From Figure 7, it is evident that the initiation of fishing bans in each zone resulted in a decrease in the number of boat detections. Additionally, the lifting of fishing bans appears to increase the number of boat detections across all four regulatory zones.

The nonparametric RD estimates by zone reported in Table 5 confirm that the starts of fishing bans have large, negative, and statistically significant (at the 1%) on boat detections. The impacts are largest on for Zone 4 in the South China Sea, reducing boat detections by 4,255. The nonparametric RD estimates reported in the second columns are all positive and have similar magnitudes to the negative effects of starting the fishing ban in the same zone. However, only estimates from Zone 2 and Zone 4 are significant at the 1% level.

Table 5: Nonparamatric RD Estimates of Fish Ban on the Number of Boats Detected

	Fishing Ban On	Fishing Ban Off
	Zone 1	
Δ Boats	-1267.057***	875.438
	(329.998)	(650.532)
	Zone 2	
Δ Boats	-2100.012***	3570.517***
	(611.860)	(1024.851)
	Zone 3	
Δ Boats	-587.244***	910.575
	(122.386)	(577.140)
	Zone 4	
Δ Boats	-4254.652***	3157.552***
	(721.291)	(994.079)
Number of Observations	151	151

Notes: This table reports the nonparametric RD estimates of fish ban on the number of boat detections, Δ Boats. The left column reports LATEs of the start of fishing bans. The right column reports LATEs of the lifting of fishing bans. Panels 1 to 4 from the top represent estimates for Zones 1 to 4 respectively.
* $p < 0.10$; ** $p < 0.05$; *** $p < 0.01$.

5 EEZ Incursions

Up to this point, my findings indicate that fishing bans reduce the number of boat detections in the Chinese EEZ. However, it's essential to note that not all boats operating within the Chinese EEZ are necessarily Chinese fishing vessels. Fishing vessels from neighboring countries may engage in illegal fishing within the Chinese EEZ, and conversely, Chinese fishing vessels may operate in the EEZs of neighboring countries.

Countries often have varying preferences for domestic seafood, especially fresh seafood, and their fishing industries can differ significantly in terms of capability and productivity. If EEZ fishing rights are effectively enforced, ensuring that only a country's fishermen exclusively exploit its EEZ, we might observe a discontinuous change in the number of boat detections at the border of two countries' EEZs.

To investigate whether this is the case, I have plotted two spatial RD graphs. In these graphs, the running variable is the distance to the outward boundary of the Chinese EEZ, and the outcome variable is the density of boat detentions.

First, I present a spatial RD graph in Figure 8 for the Chinese EEZ's outward boundary, excluding the China-Vietnam segment. Then, in Figure 9, I present a similar graph but for the China-Vietnam EEZ border. You can refer to Figure 2 for the locations of these segments.

The Gulf of Tonkin, known as Beibu Bay in China, is divided with the Vietnamese EEZ in the west and the Chinese EEZ in the east. Despite the relatively short length of the China-Vietnam EEZ border, this area experiences intense fishing activity, as indicated by Figure 4 and Figure 3. Population density is high along the nearby Chinese coasts, and even higher along the Vietnamese coasts. Notably, Hanoi and Hai Phong, the first and third most populous cities in Vietnam, are in close proximity to the Gulf of Tonkin. The average distance between the Vietnamese shore and the Chinese shore in the Gulf of Tonkin is less than 250 km (approximately 155 miles).

As we will see in Figure 8 and Figure 9, an important asymmetry distinguishes these two EEZ boundary segments.

To measure boat density, I aggregate the number of boat detections within a grid

Figure 8: Boat Density around the Chinese EEZ Outward Boundary Excluding the China-Vietnam Segment

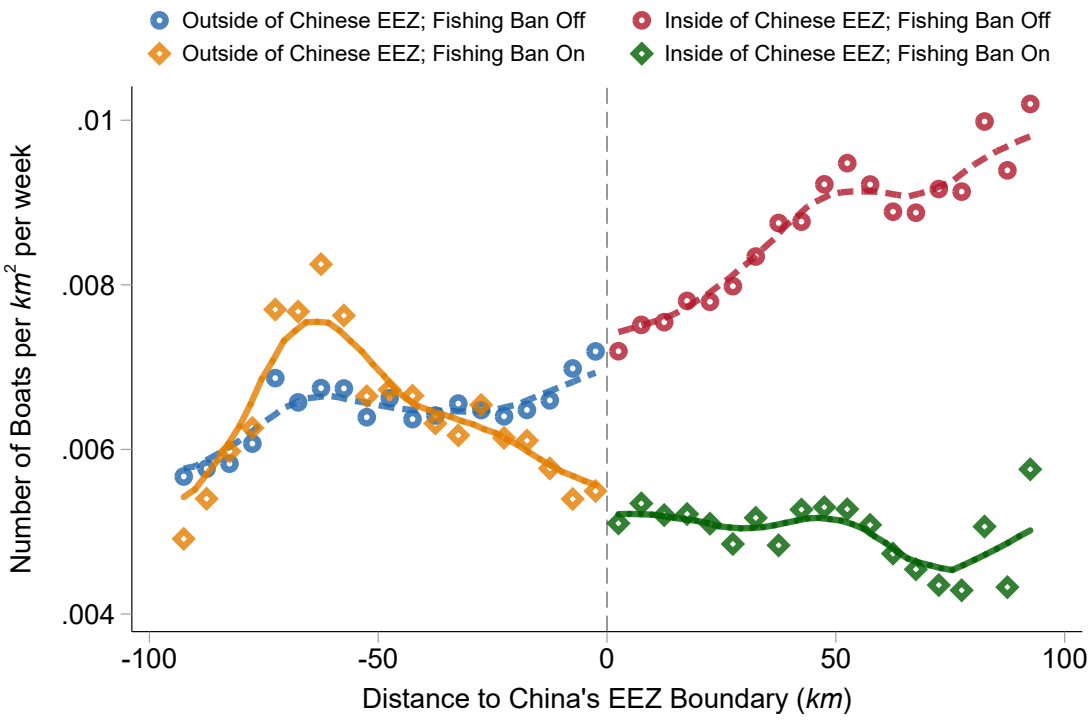

composed of numerous 5 km × 5 km cells and calculate the number of boat detections per square kilometer per week. I calculate boat density separately for periods when the Chinese fishing bans were effective in the South China Sea and periods when the bans were not in effect. Subsequently, I calculate the distances between the center of each cell and the China-Vietnam EEZ border. Cells are then averaged within distance bins of 5 km.

In Figure 8, the zero dashed line represents the China-Vietnam EEZ border projected from a 2-dimensional line onto a 1-dimensional scale. The height of a circle or a hollow diamond represents the average number of boat detections per square kilometer per week. Circles indicate boat detection rates when the Chinese fishing bans were not in effect, while hollow diamonds represent rates when the bans were enforced. Each circle or hollow diamond reflects the average within a 5-kilometer-wide distance

bin, with distance indicated on the horizontal axis.

For instance, the first circle to the right of zero represents cells with centers inside the Chinese EEZ, and their distance to the China-Vietnam EEZ border falls between 0 and 5 km. The second circle to the right of the vertical dashed line at zero represents the average boat density rate for cells located 5 km to 10 km away from the China-Vietnam EEZ border, on the side of the Chinese EEZ. The scatter plot extends up to 100 km along the horizontal axis, with each point reflecting a 5-kilometer bin.

Similarly, to the left of the zero dashed line, the horizontal value of a circle or hollow diamond, denoted as $-x$, indicates the bin averaging cells whose distance to the China-Vietnam EEZ border falls within the range $[-x - 2.5, -x + 2.5)$, for values of x such as 2.5, 7.5, and so on, up to 97.5.

If we examine the circles in Figure 8, representing boat density during periods when the fishing bans were not in effect, and the dashed lines, representing their local linear fits, a clear upward gradient becomes evident. This upward gradient suggests that when the fishing bans were lifted, sea areas closer to the Chinese continental shore had more boats detected than areas further away from the shore, and therefore, closer to the outward boundary of the Chinese EEZ.

If we were to extend the horizontal axis of Figure 8, this upward gradient would continue. This gradient confirms that, outside of the China-Vietnam segment, the Chinese EEZ tends to be more densely fished than the other side of the EEZ boundary. Furthermore, areas near the continental shore of China are more densely fished than those further offshore. However, there is no visible discontinuity at the EEZ border when the fishing bans were not in effect.

Examining the hollow diamonds, which represent the periods when fishing bans were in effect inside the Chinese EEZ, reveals no visible discontinuity at the EEZ border either. On the positive domain, i.e., the side of the Chinese EEZ, boat density during the ban periods is significantly lower than that during the no-ban periods within each distance bin. Moreover, there is no apparent upward gradient; if anything, the gradient appears to be slightly downward. These comparisons suggest that fishing bans were effective in reducing the number of detected boats in the Chinese EEZ around its

outward boundary.

On the negative domain, i.e., just outside of the Chinese EEZ, boat density is significantly lower within 25 km of the EEZ border. The absence of a discontinuity in both periods implies that the decrease in boat density inside the Chinese EEZ during the ban periods is similar to the decrease in boat density just outside of the Chinese EEZ during the same periods. As one moves farther away from the border outward (leftward in Figure 8), the density gap between the ban-off and ban-on periods narrows.

Given that the Chinese EEZ was more intensively fished during the ban-off periods compared to neighboring EEZs, the density gap between these periods just outside the Chinese EEZ suggests that Chinese fishermen may not have strictly adhered to fishing limits imposed by the EEZ boundary. The absence of a discontinuity at the EEZ border during both the fishing ban and non-ban periods also implies that fishing limits set by the EEZ border have not been consistently followed. It is unsurprising, considering the vast expanse of open ocean, the difficulties in patrolling, and the lack of advanced GPS systems on small fishing vessels to precisely determine and monitor their location relative to the EEZ border, that the EEZ border fails to create a spatial discontinuity in fishing activities.

Next, I present the spatial RD graph for the China-Vietnam EEZ border in Figure 9. Once again, circles indicate the ban-off period. Around the China-Vietnam EEZ border, the Vietnamese EEZ exhibited a higher boat density, which is in contrast to the other EEZ border segment. Moreover, at least within the Chinese EEZ and the Vietnamese EEZ close to the border, there is a downward gradient. This confirms that the Vietnamese side is more intensively fished than the Chinese side. Nevertheless, there is still no clear, discontinuous change in boat density at the border.

When we examine the hollow diamonds, representing boat density during the ban-on period, on the Vietnamese side (negative domain), the distance-density local polynomial fit is similar to that during the ban-off period, except at a higher level. It is interesting to note that the two boat density curves along the distance to the EEZ border on the Vietnamese side, i.e., the ban-off curve and ban-on curve, appear to parallel each other.

Figure 9: Boat Density around the China-Vietnam EEZ Boundary

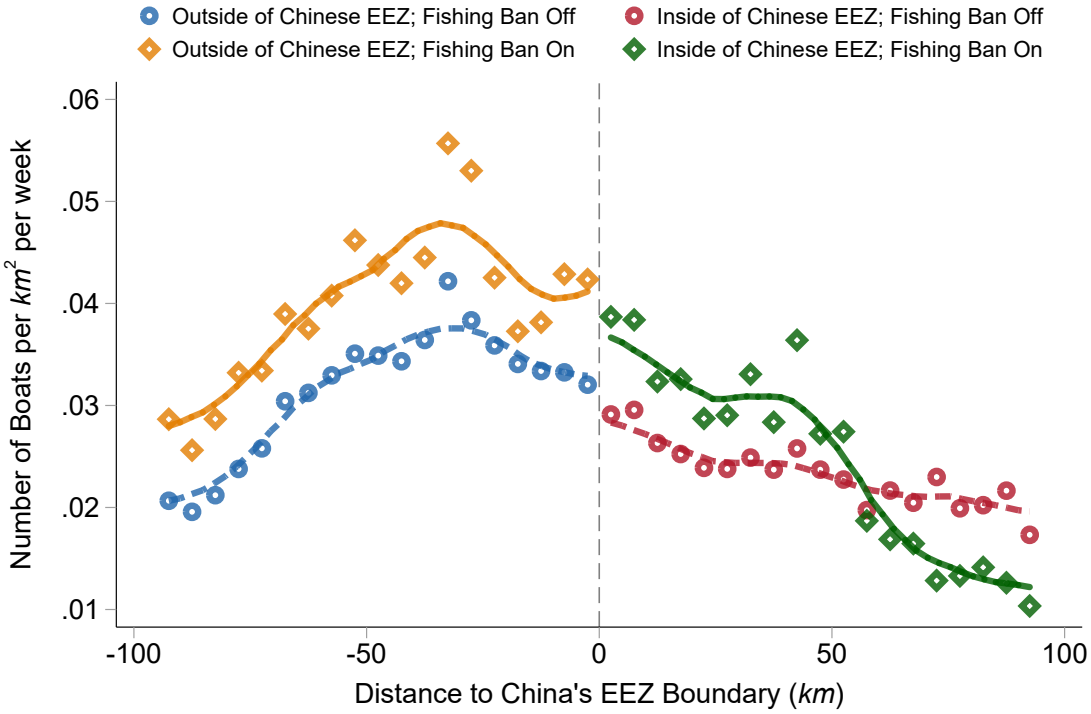

However, on the Chinese side (positive domain), within 50 km from the border, the boat density during the banned periods is higher than that during the no-ban periods. Beyond 50 km from the border, closer to the Chinese shore, the boat density during the banned periods falls below the boat density during the no-ban period. This pattern suggests that Vietnamese fishermen, who outnumber Chinese fishermen in the Gulf of Tonkin, may not have strictly adhered to the EEZ demarcation.

To formally test the existence of a spatial discontinuity in boat density at the China-Vietnam EEZ border, I estimate the boat density on both sides of the border using a simple local polynomial density estimator proposed by Cattaneo et al. (2020). My focus is on the boat density during the fishing ban period. To simplify the problem from two dimensions to one dimension, I define the running variable as the distance between a location in the Gulf of Tonkin and the China-Vietnam EEZ border.

The simple local polynomial density estimator by Cattaneo et al. (2017) serves a

similar objective to the density test by McCrary (2008). However, the Cattaneo et al. (2017) estimator does not require pre-binning of the data, eliminating the need to specify the bin width as an additional tuning parameter.

In Figure 10, I present the local polynomial estimates of boat density during fishing ban periods around the China-Vietnam EEZ border, along with their 95% confidence intervals using the Jackknife method. As evident from the RD graph, there is no discernible discontinuity in boat density during the fishing ban at the China-Vietnam EEZ border. A test for the discontinuity in density yields a p-value of 0.55.

Figure 10: Spatial Continuity of Boat Density around the China-Vietnam EEZ Boundary

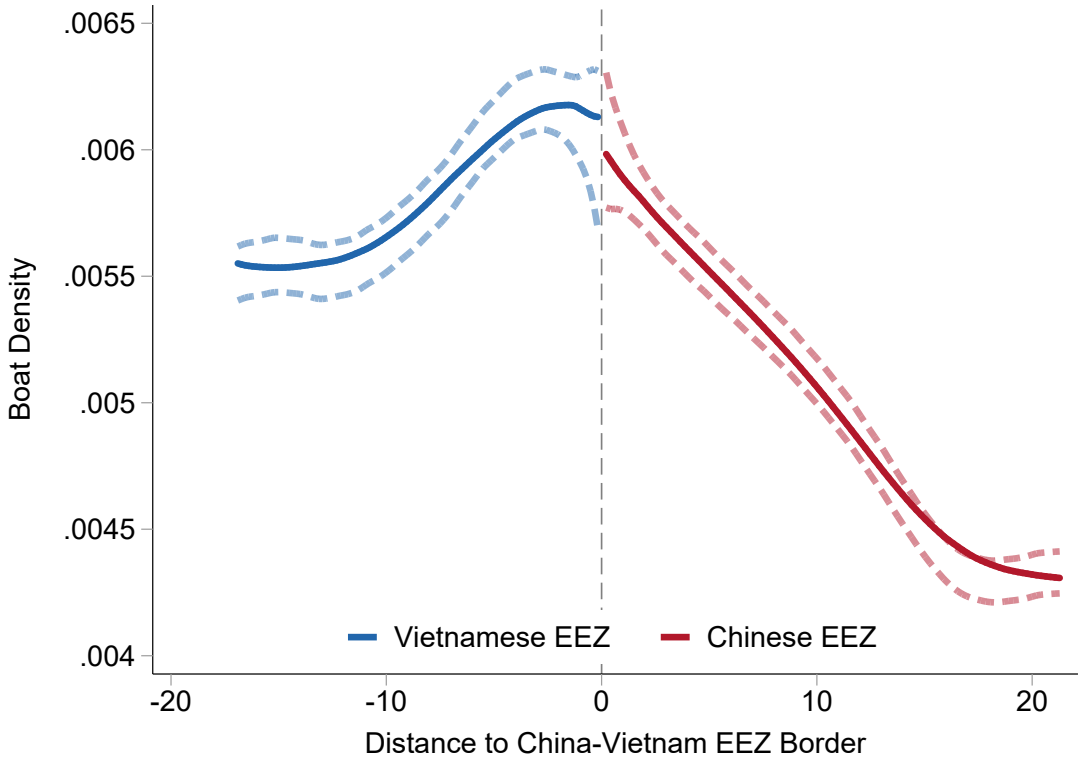

Collectively, Figure 8, Figure 9, and Figure 10 suggest that Chinese fishermen operate outside of the Chinese EEZ and fish in most of their neighbors' EEZs, except for Vietnam's, during the ban-off period. Additionally, Vietnamese fishermen sail into the Chinese EEZ during the Chinese summer fishing ban, thereby benefiting from the Chinese

fishing bans by accessing less crowded fishing grounds near their border. These findings align with prior research indicating the presence of substantial spatial spillovers and inter-jurisdictional externalities in pollution and environmental policies (see, e.g., Burgess et al., 2012; Kahn et al., 2015; Lipscomb and Mobarak, 2016).

6 Concluding Remarks

There may have been more efficient market-based systems for fishery management than a command-and-control approach, such as seasonal fishing bans (Weninger and Waters, 2003; Stavins, 2003). For example, New Zealand has implemented a system of transferable fishing quotas (Newell et al., 2005).

However, the cost-effectiveness of a tradable permit system may be substantially dampened by transaction costs in market-based systems, particularly in the context of global environmental preservation that requires the cooperation of sovereign nations (Stavins, 1995; Libecap, 2014). More importantly, developing countries typically have limited capacity for implementing complex regulatory regimes, monitoring compliance, adjudicating disputes, and enforcing regulation. Under various institutional constraints, a command-and-control method may be more practical.

To support the recovery of fishing stocks and promote sustainable fisheries, China has annually implemented a large-scale fishing ban during the summer. This paper provides evidence that China's seasonal fishing bans significantly reduced fishing activities in the Chinese EEZ when they were in effect. These findings imply that when properly implemented, seasonal fishing bans can be an effective tool for achieving sustainable fisheries.

First, the Chinese experience demonstrates that the successful enforcement of fishing bans relies on complementary measures, including offshore patrols, inspections of fish markets, licensing and registration management of fishing vessels, and the availability of transfer payments during the ban periods.

Second, China has witnessed rapid growth in aquaculture over the past two decades and has become one of the largest exporters of farmed fish. The presence

of farmed fish as substitutes for domestic consumers may have reduced the incentives for fishermen to evade fishing bans in order to supply seafood during the ban periods.

Third, China boasts one of the largest and contiguous Exclusive Economic Zones (EEZs) due to its extensive coastline. For other countries considering similar fishing bans, effective fishery policy-making may necessitate coordination with neighboring countries that share EEZ borders. Fishermen from neighboring countries may exploit one country's fishing bans, as evidenced by the potential EEZ incursions found in this study. Moreover, neighboring countries often share regional fishing stocks, and these inter-jurisdictional spillovers could potentially undermine the effectiveness of fishing bans implemented by a single country. Even within a jurisdiction, inter-regional spillovers can pose challenges to the enforcement of fishing bans. There have been reports of fishing vessels in ports where fishing bans are not yet in effect traveling to zones where fishing bans are already in place. This issue prompted the Ministry of Agriculture to synchronize the starting dates of the bans across all zones of the Chinese EEZ in 2017.

Finally, the distribution of size, power, range, and capacity of commercial fishing vessels is likely to be crucial in designing and implementing an optimal seasonal fishing ban. Further studies analyzing the heterogeneous impacts of fishing bans on different vessels and their spatial distribution should provide valuable insights into the design of effective fishery management strategies.

References

Anderson, Michael L (2014) "Subways, Strikes, and Slowdowns: the Impacts of Public Transit on Traffic Congestion," *American Economic Review*, 104 (9), 2763–96.

Assunção, Juliano, Clarissa Gandour, and Romero Rocha (2023) "DETER-ing Deforestation in the Amazon: Environmental Monitoring and Law Enforcement," *American Economic Journal: Applied Economics*, 15 (2), 125–56.

Auffhammer, Maximilian and Ryan Kellogg (2011) "Clearing the Air? The Effects of Gasoline Content Regulation on Air Quality," *American Economic Review*, 101 (6), 2687–2722.

Axbard, Sebastian (2016) "Income Opportunities and Sea Piracy in Indonesia: Evidence from Satellite Data," *American Economic Journal: Applied Economics*, 8 (2), 154–94.

Besley, Timothy, Thiemo Fetzer, and Hannes Mueller (2015) "The Welfare Cost of Lawlessness: Evidence from Somali Piracy," *Journal of the European Economic Association*, 13 (2), 203–239.

Brown, Gardner M (2000) "Renewable Natural Resource Management and Use Without Markets," *Journal of Economic Literature*, 38 (4), 875–914.

Burgess, Robin, Matthew Hansen, Benjamin A. Olken, Peter Potapov, and Stefanie Sieber (2012) "The Political Economy of Deforestation in the Tropics," *Quarterly Journal of Economics*, 127 (4), 1707–1754, 10.1093/qje/qjs034.

Calonico, Sebastian, Matias D Cattaneo, and Rocio Titiunik (2014) "Robust Nonparametric Confidence Intervals for Regression-Discontinuity Designs," *Econometrica*, 82 (6), 2295–2326.

Carruthers, Bruce G and Naomi R Lamoreaux (2016) "Regulatory races: the effects of jurisdictional competition on regulatory standards," *Journal of Economic Literature*, 54 (1), 52–97.

Cattaneo, Matias D., Michael Jansson, and Xinwei Ma (2017) "Simple local regression distribution estimators with an application to manipulation testing," *Working Paper*.

Cattaneo, Matias D, Michael Jansson, and Xinwei Ma (2020) "Simple Local Polynomial Density Estimators," *Journal of the American Statistical Association*, 115 (531), 1449–1455.

Chan, H Ron and Christy Zhou (2023) "Charged Up? Distributional Impacts of Green Energy on Local Labor Markets," *SSRN WOrking Paper*, `https://papers.ssrn.com/sol3/papers.cfm?abstract_id=4534479`.

Chan, H Ron and Yichen Christy Zhou (2021) "Regulatory Spillover and Climate Cobenefits: Evidence From New Source Review Lawsuits," *Journal of Environmental Economics and Management*, 110, 102545.

Chen, Yihsu and Alexander Whalley (2012) "Green Infrastructure: The Effects of Urban Rail Transit on Air Quality," *American Economic Journal: Economic Policy*, 4 (1), 58–97.

China Fishery Statistical Year Book (2016) *China Fishery Statistical Year Book*: China Agriculture Press.

Cropper, Maureen L and Wallace E Oates (1992) "Environmental Economics: A Survey," *Journal of Economic Literature*, 30 (2), 675–740.

Davis, Lucas W. (2008) "The Effect of Driving Restrictions on Air Quality in Mexico City," *Journal of Political Economy*, 116 (1), 38–81.

Donaldson, Dave and Adam Storeygard (2016) "The View from Above: Applications of Satellite Data in Economics," *Journal of Economic Perspectives*, 30 (4), 171–98.

Elvidge, Christopher D, Kimberly E Baugh, Mikhail Zhizhin, and Feng-Chi Hsu (2013) "Why VIIRS Data Are Superior to Dmsp for Mapping Nighttime Lights," *Proceedings of the Asia-Pacific Advanced Network*, 35, 62–69.

Elvidge, Christopher D, Mikhail Zhizhin, Kimberly Baugh, and Feng-Chi Hsu (2015a) "Automatic Boat Identification System for VIIRS Low Light Imaging Data," *Remote Sensing*, 7 (3), 3020–3036.

Elvidge, Christopher D, Mikhail Zhizhin, Kimberly Baugh, Feng-Chi Hsu, and Tilottama Ghosh (2015b) "Methods for Global Survey of Natural Gas Flaring from Visible Infrared Imaging Radiometer Suite Data," *Energies*, 9 (1), 14.

FAO (2002) "Fishery Statistics: Reliability and Policy Implications," *memorandum*.

Flückiger, Matthias and Markus Ludwig (2015) "Economic Shocks in the Fisheries Sector and Maritime Piracy," *Journal of Development Economics*, 114, 107–125.

Hausman, Catherine and David S Rapson (2018) "Regression Discontinuity in Time: Considerations for Empirical Applications," *Annual Review of Resource Economics*, 10, 533–552.

He, Guojun, Shaoda Wang, and Bing Zhang (2020) "Watering Down Environmental Regulation in China," *Quarterly Journal of Economics*, 135 (4), 2135–2185.

Henderson, J. Vernon, Adam Storeygard, and David N. Weil (2012) "Measuring Economic Growth from Outer Space," *American Economic Review*, 102 (2), 994–1028, 10.1257/aer.102.2.994.

Hodler, Roland and Paul A. Raschky (2014) "Regional Favoritism," *Quarterly Journal of Economics*, 129 (2), 995–1033, 10.1093/qje/qju004.

Kahn, Matthew E, Pei Li, and Daxuan Zhao (2015) "Water Pollution Progress at Borders: the Role of Changes in China's Political Promotion Incentives," *American Economic Journal: Economic Policy*, 7 (4), 223–42.

Libecap, Gary D (2014) "Addressing Global Environmental Externalities: Transaction Costs Considerations," *Journal of Economic Literature*, 52 (2), 424–479.

Lipscomb, Molly and Ahmed Mushfiq Mobarak (2016) "Decentralization and Pollution Spillovers: Evidence from the Re-Drawing of County Borders in Brazil," *Review of Economic Studies*, 84 (1), 464–502.

McCrary, Justin (2008) "Manipulation of the Running Variable in the Regression Discontinuity Design: A Density Test," *Journal of Econometrics*, 142 (2), 698–714.

Michalopoulos, Stelios and Elias Papaioannou (2013) "National Institutions and Subnational Development in Africa," *Quarterly Journal of Economics*, 129 (1), 151–213.

Ministry of Agriculture (2017) "Most Restrictive Fishing Conservation Policy Protects Marine Fishery Resources," *Press Office of the Chinese Ministry of Agriculture*, `http://jiuban.moa.gov.cn/zwllm/zwdt/201708/t20170803_5768337.htm`.

Newell, Richard G, James N Sanchirico, and Suzi Kerr (2005) "Fishing Quota Markets," *Journal of Environmental Economics and Management*, 49 (3), 437–462.

Newey, Whitney K. and Kenneth D. West (1986) "A Simple, Positive Semi-definite, Heteroskedasticity and Autocorrelation Consistent Covariance Matrix," *Econometrica*, 55 (3), 703–08.

Sigman, Hilary (2002) "International Spillovers and Water Quality in Rivers: Do Countries Free Ride?" *American Economic Review*, 92 (4), 1152–1159.

Stavins, Robert N (1995) "Transaction Costs and Tradeable Permits," *Journal of Environmental Economics and Management*, 29 (2), 133–148.

——— (2003) "Experience With Market-Based Environmental Policy Instruments," in *Handbook of Environmental Economics*, 1, 355–435: Elsevier.

U.N. Food and Agriculture Organization (2014) "The State of World Fisheries and Aquaculture," *FAO Fisheries and Aquaculture Department*.

——— (2016) "The State of World Fisheries and Aquaculture," *FAO Fisheries and Aquaculture Department*.

Walker, W Reed (2011) "Environmental regulation and labor reallocation: Evidence from the Clean Air Act," *American Economic Review*, 101 (3), 442–447.

Watson, Reg and Daniel Pauly (2001) "Systematic Distortions in World Fisheries Catch Trends," *Nature*, 414 (6863), 534.

Weninger, Quinn and James R Waters (2003) "Economic Benefits of Management Reform in the Northern Gulf of Mexico Reef Fish Fishery," *Journal of Environmental Economics and Management*, 46 (2), 207–230.